Food & Medicine Homology

ISSN 3006-6867 (print); 3006-4252 (online)
https://doi.org/10.26599/FMH.2025.9420032

Research Article

Effect of extrusion processing on physicochemical and functional properties of water-soluble dietary fiber and water-insoluble dietary fiber of whole grain highland barley

Jing-Wen Xu (✉), Tian-Tian Tian, Yong Zhao (✉)

College of Food Science and Technology, Shanghai Ocean University, Shanghai 201306, China

Received: 1 July 2024 / **Revised:** 23 July 2024 / **Accepted:** 23 July 2024

Abstract: The effect of extrusion processing on water-soluble dietary fiber (SDF) and water-insoluble dietary fiber (IDF) of whole grain highland barley (HB) in terms of morphology, physicochemical and functional properties, and antioxidant activities was studied. Extrusion processing resulted in the more porous and loose structure of SDF and IDF, and significantly increased the specific surface area of SDF and IDF. The predominant monosaccharide in IDF and SDF was cellulose. Extrusion processing improved the water holding capacity of SDF and IDF by 23.9% and 40.4%, respectively. The glucose absorption capacity and glucose dialysis retardation index of IDF and SDF were further significantly improved by extrusion processing, indicating the great potential of glucose control *in vitro* of IDF and SDF. The cholesterol adsorption capacity, nitrite adsorption capacity, and cation exchange capacity of IDF and SDF were also significantly improved through extrusion processing. Extrusion processing significantly improved the antioxidant activities of IDF and SDF which reflected as the improved DPPH and $ABTS^+$ scavenging activities. Taken together, extrusion processing improved the physicochemical and functional properties of dietary fiber of whole grain HB, as well as the antioxidant activities. This study showed the great potential of dietary fiber of whole grain HB in the applications of functional foods for improving the health benefits.

Keywords: whole grain; highland barley; extrusion; dietary fiber; health benefits

Citation: Xu J. W., Tian T. T., Zhao Y. Effect of extrusion processing on physicochemical and functional properties of water-soluble dietary fiber and water-insoluble dietary fiber of whole grain highland barley. *Food & Medicine Homology*, 2025, 2: 9420032. https://doi.org/10.26599/FMH.2025.9420032

1 Introduction

Epidemiological studies have been shown the inadequate intake of whole grains was the predominant dietary factor leading to the chronic disease and death[1]. Highland barley (HB, *Hordeum vulgare*), also known as "Qingke" in Chinese, is mainly cultivated and grown in high-altitude of 4,200-4,500 m in Tibet areas[2]. HB has been attracted increasing attention due to its nutritional profile such as high content of dietary fiber (DF, 8.16-21.46%) and health-promoting functions[3]. Dietary fiber, referred to non-starch polysaccharides and seventh nutrition for humans, is resistant to digestion and absorption in GI tract, but can be fermented by the microorganisms in the large intestine. Moderate intake of DF is known to be associated with reduced risk of many chronic diseases such as coronary heart disease, cardiovascular disease, diabetes, and colon cancer[4].

Extrusion technology is known to possess the functions of mixing, shearing, kneading, cooking, and compression at high temperature and high pressure[5]. Extrusion technology has been widely employed for cereal grains processing for improving the properties, qualities, and health benefits[6]. Currently, studies have been focused on the effect of extrusion processing on physicochemical and functional properties of dietary fibers[7]. However, little is known about the extrusion processing on the structure-function relationship between the dietary fiber and their functional characteristics and antioxidant activities. To our knowledge, there was no available study yet about the effect of extrusion processing on the analysis of monosaccharide composition, physicochemical properties, functional properties, and antioxidant activities of IDF and SDF of whole grain highland barley.

Therefore, the aim of this study was to focus on the monosaccharide composition of SDF and IDF extracted from whole grain HB before and after extrusion processing, and evaluation of physicochemical and functional properties, and antioxidant activities of SDF and IDF. This study was expected to provide insights of extrusion processing on SDF and IDF of HB in terms of physiochemical and functional properties, and promote the potential applications of SDF and IDF of HB in functional foods.

Address correspondence to Jing-Wen Xu, jw-xu@shou.edu.cn; Yong Zhao, yzhao@shou.edu.cn

2 Materials and methods

2.1 Materials

White highland barley (*Hordeum vulgare* var. *Coeleste* L. Himalayan 22) was purchased from Beijing Yihe Guxiang Co., Ltd. (Beijing, China). Chemicals including sodium hydroxide, Congo red, sodium nitrite, aluminium nitrate, glacial acetic acid, sodium phosphate, pepsin, trypsin and glucose were purchased from Sinopharm Group Chemical Reagent Co., Ltd. (Shanghai, China). Sodium carbonate and sodium dihydrogen phosphate were purchased from Shanghai Acmec Biochemical Co., Ltd. (Shanghai, China). Phloroglucinol was purchased from Shanghai Hanhong Scientific Co., Ltd. (Shanghai, China). Hydrochloric acid, propyl alcohol and sulfuric acid were purchased from Shanghai Lingfeng Chemical Reagent Co., Ltd. (Shanghai, China). Ethyl alcohol was purchased from Sangon Biotech Co., Ltd. (Shanghai, China). *p*-Hydroxybenzenesulfonic acid and *α*-glucosidase hydrogen peroxide were purchased from Shanghai Macklin Biochemical Co., Ltd. (Shanghai, China). Sodium hydrogen phosphate was purchased from Shanghai Ziding Biochemical Scientific Co., Ltd. (Shanghai, China).

2.2 Extrusion processing of HB and extraction of SDF and IDF

Whole grain HB was processed through extruder (Cobelon CTE-35, Cobelon Machinery Co., Ltd, Shanghai, China). The moisture content of HB flour was adjusted to 23%. Screw speed and barrel temperature was 130 r/min and 107 °C, respectively. The extraction of SDF and IDF was followed the method of AOAC 991.43. Briefly, one gram of highland barley powder before and after extrusion processing and 25 mL of phosphate buffer solution (0.1 mol/L, pH 6) were mixed in beaker. And 100 mL of thermostable *α*-amylase enzyme were placed in magnetic stirrer (LC-DMS-H, Shanghai Lichen Bangxi Instrument Technology, Co., Ltd. Shanghai, China) at 400 r/min for 15 min and then cooled to the room temperature. The pH was adjusted to 9.5. The mixture was mixed with 0.1 g of alkaline protease and stirred at 40 °C for 1 h. After cooling, the pH was adjusted 4.0. Subsequently, 0.1 g of glucoamylase was added to mixture, stirred at 60 °C for 30 min, and then heated in a 100 °C water bath for 10 min. The mixture was centrifuged at 4,000 r/min for 15 min (Avanti J-26XP Centrifuge, Beckman Coulter Trading Co., Ltd. Beckman Coulter, USA). The residue was washed with 75% ethanol (*v*/*v*), 95% ethanol (*v*/*v*) and acetone, respectively, to achieve the IDF. The supernatant was evaporated and washed with 75% ethanol (*v*/*v*), 95% ethanol (*v*/*v*) and acetone, respectively, to achieve the SDF. The raw IDF and extruded IDF was named as RIDF and EIDF. The raw SDF and extruded SDF was named as RSDF and ESDF.

2.3 Analysis of monosaccharide composition of SDF and IDF

The monosaccharide composition of was measured followed the method of Xi *et al.*[2] by using ion-exchange chromatography (ICS 5000+, Thermo Fisher Scientific Co., Ltd. Shanghai, China). Briefly, 0.2 g of sample was dissolved with 100 mL of trifluoroacetic acid (2 mol/L), heated at 121 °C for 2 h, washed with methanol (99.99%, *v*/*v*/*v*) and dried under flowing of nitrogen. The analysis conditions were as follows: HPLC column: Dionex™ CarboPac™ PA20 (150 × 5.0 mm, 10 μm); injection volume: 5 μL; mobile phase A: sterile water; mobile phase B: 0.1 mol/L of NaOH; mobile phase C: 0.1 mol/L NaOH and 0.2 mol/L NaAC; the flow rate: 0.5 mL/min. The column temperature was 30 °C. The gradient elution program was: 0 min, A/B/C (95:5:0, *v*/*v*/*v*); 26 min, A/B/C (85:5:10, *v*/*v*/*v*); 42 min A/B/C (85:5:10, *v*/*v*/*v*); 42.1 min, A/B/C (60:0:40, *v*/*v*/*v*); 52 min, A/B/C (60:40:0, *v*/*v*/*v*); 52.1 min A/B/C (95:5:0, *v*/*v*/*v*); 60 min, A/B/C (95:5:0, *v*/*v*/*v*).

2.4 Physicochemical properties of SDF and IDF of HB

2.4.1 *Scanning electron microscopy (SEM)*

The surface morphology was determined by SEM (Hitachi SU5000, Hitachi, Tokyo, Japan). Each sample was sprayed with gold before analysis. The test was observed at a 5 kV accelerated voltage.

2.4.2 *Particle size analysis and specific surface area*

The particle size and specific surface area (SSA) of the samples were measured using Laser Particle Size Analyzer (MasterSizer 2000, Malvern Instrument, Co., Ltd, Malvern, UK). The dispersing medium was distilled water. The refractive indices of dispersants and samples were 1.33 and 1.53, respectively, and the shading parameter was 10%-20%. SSA was the equivalent value calculated by the software, assuming that the powder particles are solid spheres[8].

2.4.3 *Fourier transform infrared spectroscopy (FTIR)*

The structural analysis of HB was analyzed through FTIR spectrometer (PerkinElmer Spotlight 400, Shanghai Renhe Scientific Instrument Co., Ltd. Shanghai, China). Each sample was coated with potassium bromide and pressed into slice of 1.0 mm. The test was performed at the resolution of 0.09 cm^{-1} in the range of 4,000-400 cm^{-1}.

2.4.4 *Thermogravetic property*

The thermogravetic property of dietary fiber was evaluated by using Thermogravimetric Analyzer (TGAQ50, TA Instruments, New Castle, USA). Five gram of sample was placed in an aluminum sample pan and heated from 25-600 °C at the heating rate of 10 °C under flowing nitrogen of 50 mL/min. Each test was repeated for three replicates.

2.4.5 *Water holding capacity (WHC) and oil holding capacity (OHC)*

WHC and OHC was followed by the previous method of Niu *et al.*[9] with modifications. For WHC: 1 g of sample was mixed with 20 mL of DI water for 12 h. The mixture was centrifuged at 4,000 r/min for 25 min (Avanti J-26XP Centrifuge, Beckman Coulter Trading Co., Ltd. Beckman Coulter, USA). The precipitates were collected and weighed. WHC was calculated as the following:

$$\mathrm{WHC(g/g)} = \frac{M_1 - M_2}{M_3} \quad (1)$$

Wherein, M_1 was the mass of sample along with the centrifuge tube after soaking (g); M_2 was the mass of the centrifuge tube (g); M_3 was the dry mass of sample (g).

For OHC: 2.5 g of sample was mixed with 4 g of soybean oil. The sample was sealed and incubated in 37 °C water batch for 4 h. Then the mixture was centrifuged at 4,000 r/min for 15 min to obtain the precipitation. OHC was calculated as the following:

$$\mathrm{OHC(g/g)} = \frac{M_2 - M_1}{M_1} \quad (2)$$

Wherein, M_1 was the original mass of the sample (g); M_2 was the mass of the oil-holding sample (g). Each test was repeated for three replicates.

2.5 Functional properties

2.5.1 *Glucose adsorption capacity (GAC) and glucose dialysis retardation index (GDRI)*

The GAC and GDRI were determined according to the method of Zheng *et al.*[10] and Gu *et al.*[11] with modifications, respectively.

For GAC: 1 g of sample was mixed with 100 mL of glucose solution of different concentration (10, 50, 100, and 200 mg/mL). The mixture was stirred at 37 °C for 5 h using magnetic stirrer (LC-DMS-H, Shanghai Lichen Bangxi Instrument Technology, Co., Ltd. Shanghai, China) and centrifuged at 4,000 r/min for 20 min. The glucose content in the supernatant was determined by DNS colorimetry. The glucose solution without DF sample was used as a blank control. GAC was calculated as the follows:

$$\mathrm{GAC(mmol/g)} = \frac{(C_0 - C_1)}{M} \quad (3)$$

Wherein, C_0 represented the glucose concentration (mmol/L) in the solution before adsorption; C_1 represented the glucose concentration (mmol/L) in the supernatant of after adsorption; M represented the sample mass (g).

For GDRI: 1 g of sample was added to 25 mL of glucose solution (100 mmol/L), stirred at 37 °C for 1 h. The mixture was transferred into a dialysis bag (Mw=10,000 Da) and placed in DI water and stirred at 37 °C for 1 h. The glucose content of the dialysate was collected and measured at time of 30 and 60 min, respectively. A glucose solution without DF was used as control. The GDRI was calculated as the follows:

$$\mathrm{GDRI}(\%) = \left(1 - \frac{M}{N}\right) \times 100 \quad (4)$$

Wherein, M represented the dialyzed concentration (mmol/L) of glucose in the sample; N was the dialyzed concentration (mmol/L) of glucose in the control sample. Each test was repeated for three replicates.

2.5.2 *Inhibitory activities of α-amylase and α-glucosidase*

The inhibitory activities of α-amylase and α-glucosidase were measured according to the method of Chen *et al.*[12]. For α-amylase inhibition rate: 500 mL of DF (20 mg/mL) of and 500 mL of α-amylase (1 U/mg) were incubated in the water bath at 37 °C for 10 min. The mixture was added 500 mL potato starch solution (1%, *w/v*) for another 10 min of incubation at 37 °C. The reaction was terminated by adding 1 mL of DNS and boiled in water path for 5 min. After cooling down, the mixture was diluted with 9 mL of DI water and measured at 520 nm. Buffer without DF was used as the reference control. The inhibitory activity of α-amylase was analyzed as the following:

$$\alpha\text{-amylase inhibitory rate}(\%) = \frac{Ac - As}{Ac} \times 100 \quad (5)$$

Wherein, *Ac* and *As* was the glucose content in the control and in the sample, respectively.

For α-glucosidase inhibition rate: 50 μL of DF (20 mg/mL) was mixed with 100 μL PBS (100 mmol/L) and 0.2 mL of α-glucosidase (0.5 U/mL). The mixture was incubated in a water bath at 37 °C for 10 min, and then was mixed with 0.4 mL of PNPG (1.5 mmol/L). The reaction was terminated by adding 1 mL of 1 mol/L of sodium carbonate after 30 min of incubation at 37 °C. The mixture was measured at 400 nm. The inhibitory activity of α-glucosidase was analyzed as the following:

$$\alpha\text{-glucosidase inhibitory rate}(\%) = \frac{Ac - As}{Ac} \times 100 \quad (6)$$

Wherein, *Ac* and *As* was the glucose content in the control and in the sample, respectively.

2.5.3 *Cholesterol adsorption capacity (CAC)*

The CAC was measured according to the method of Niu *et al.*[9] with modifications. One gram of sample was mixed with 25 mL of diluted yolk solution (1:9, *v/v*) and the pH was adjusted to 2 or 7 to simulate the gastric and intestinal environment, respectively. The mixture was shaken at 37 °C for 3 h and then centrifuged at 4,000 r/min for 20 min (Avanti J-26XP Centrifuge, Beckman Coulter Trading Co., Ltd. Beckman Coulter, USA). The supernatant was collected and the cholesterol concentration in the supernatant was determined by the *o*-phthalaldehyde method. The egg yolk solution without fiber sample was used as the control reference. CAC was calculated as the following equation:

$$\mathrm{CAC(mg/g)} = \frac{C_1 - C_2}{M_0} \quad (7)$$

Wherein, C_1 represented the cholesterol content (mg) in the egg yolk (mg/mL) before adsorption; C_2 represented the cholesterol content (mg) in the supernatant after the adsorption; M_0 represented the sample mass (g).

2.5.4 *Nitrite adsorption capacity (NIAC)*

The NIAC was determined according to the method of Zheng *et al.*[13] with modifications. One gram of DF was mixed with 50 mL of $NaNO_2$ solution (20 μg/mL) to adjust pH to 2 or 7 to simulate the gastric or intestinal environment, respectively. The mixture was oscillated at 37 °C for 20 min and centrifuged at 4,800 r/min for 10 min for collecting the supernatant. The nitrite ion concentration was determined by the N-1-naphthylethylenediamine dihydrochloride method. The sample system without DF was used as the control. NIAC was calculated as the following:

$$\mathrm{NIAC(\mu g/g)} = \frac{C_1 - C_2}{W} \times V \quad (8)$$

Wherein, C_1 (μg/mL) and C_2 (μg/mL) represented the nitrite ion content in the supernatant after and before adsorption, respectively; W represented the sample mass (g); V was the volume of reaction solution (mL).

2.5.5 *Cation exchange capacity (CEC)*

CEC was followed by the method of Yan *et al.*[14] with modifications. One gram of sample was added to 30 mL of HCl (0.1 mol/L) at 37 °C for 12 h for acidification. After filtration, the precipitate was washed by adding a drop of $AgNO_3$ (concentration of 20%), till no precipitate was formed. Then the precipitate was dried at 50 °C for 12 h. The DF sample was suspended in DI water, followed by the addition of 2-3 drops of phenolphthalein, and then titrated with 25 mmol/L NaOH. CEC was expressed as the number of milliequivalents per gram of dry sample (mmol/g).

2.5.6 Total phenolic content (TPC)

The TPC of dietary fiber was determined using Folin-Ciocalteu reagent-based colorimetric assay. One milliliter of 20 mg/mL sample solution were mixed with 2.5 mL Folin-Ciocalteu reagent for 3 min, and then 2 mL of 7.5% (*w/v*) Na_2CO_3 at 37 °C for 2 h in dark. The absorbance was measured at 760 nm. Phenolic content was expressed as milligram of gallic acid equivalents (GAE) per gram of sample (mg GAE/g sample)[15].

2.5.7 Antioxidant capacity of SDF and IDF

The DPPH free radical scavenging ability and $ABTS^+$ free radical scavenging activity were measured according to method of Li *et al.*[16] with modifications.

DPPH radical scavenging activity: DF solution (400 mL) of various concentrations (0.5, 1, 2, 3, 4, and 5 mg/mL) was mixed with 600 mL of DPPH solution (60 mM) in methane, respectively. The mixture was shaken and incubated in dark at room temperature for 30 min, the absorbance of mixture was measured at 517 nm. The DPPH scavenging rate was calculated as follows:

$$\text{DPPH scavenging activity}(\%) = \left[1 - \frac{A_{\text{test}} - A_{\text{control}}}{A_{\text{blank}}}\right] \times 100 \quad (9)$$

Wherein, A_{test}, A_{control}, and A_{blank} was the absorbance of the test sample, control, and the blank sample, respectively.

$ABTS^+$ radical scavenging activity: DF solution (20 mL) of various concentrations (0.5, 1, 2, 3, 4, and 5 mg/mL) was mixed with 200 μL of $ABTS^+$ solution. The mixture was placed in dark for 10 min. The absorbance was determined at 734 nm with microplate reader (uQuant, Shanghai Dending International Trade Co., Ltd. Shanghai, China). The $ABTS^+$ scavenging rate was calculated as follows:

$$ABTS^+ \text{ scavenging activity}(\%) = \frac{A_{\text{blank}} - (A_{\text{supernatant}} - A_{\text{control}})}{A_{\text{blank}}} \times 100 \quad (10)$$

Wherein, $A_{\text{supernatant}}$, A_{control}, and A_{blank} was the absorbance of the test sample, control, and the blank sample, respectively.

2.6 Statistical analysis

Data was analyzed using SPSS analysis software. Statistically significant difference was evaluated through ANOVA and Duncan's test (P<0.05).

3 Results & discussion

3.1 Monosaccharide analysis of IDF and SDF

The ion-exchange chromatography of IDF and SDF was shown in Fig. 1 and the monosaccharide composition of IDF and SDF was shown in Table 1. SDF was mainly composed of glucose and arabinose. IDF was mainly composed of glucose, arabinose and xylose. This was in line with previous studies that glucose was the predominant component of cellulose, and xylose and arabinose were the major component of hemicellulose[17,18].

3.2 Physiochemical properties of IDF and SDF

3.3 Scanning electron microscopy

Microstructure of IDF and SDF was shown in Fig. 2. RIDF showed rough and spongy structure which was in line with the previous result of Xi *et al.*[2]. IDF and SDF after extrusion processing showed more porous and irregular flaky structure compared to RIDF and RSDF, which was attributed to the effect of temperature and mechanical force during extrusion processing[19].

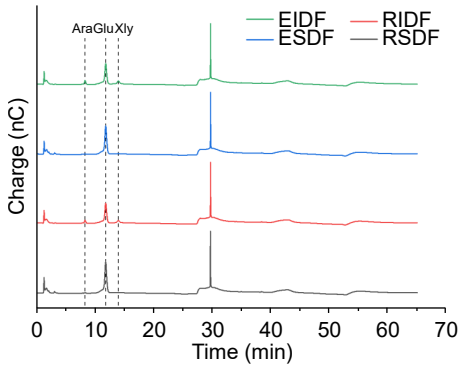

Figure 1 Ion-exchange chromatography of monosaccharide of SDF and IDF.

Table 1 Monosaccharide composition of IDF and SDF

Treatment	Arabinose (%)	Glucose (%)	Xylose (%)
RIDF	7.24 ± 0.76^b	83.42 ± 0.51^b	9.35 ± 0.25^a
EIDF	8.78 ± 0.76^a	81.27 ± 1.56^b	9.96 ± 2.32^a
RSDF	0.68 ± 0.70^c	99.32 ± 0.07^a	-
ESDF	0.99 ± 0.70^c	99.01 ± 0.07^a	-

n=3. Values were expressed mean ± SD. Different letters in the same column indicated significant difference (P < 0.05).

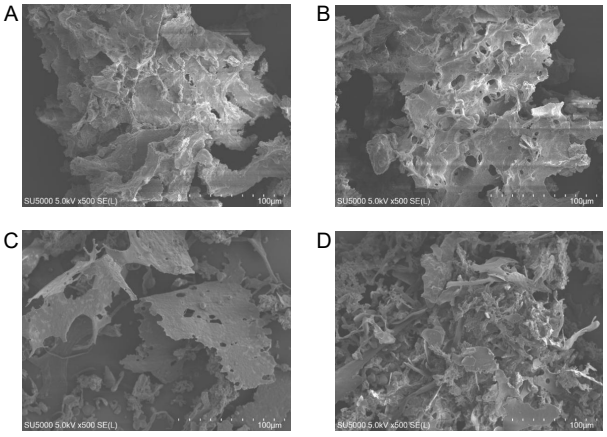

Figure 2 Microstructure of RIDF (A), EIDF (B), RSDF (C), ESDF (D).

3.3.1 Particle size and SSA

Particle size and SSA of DF were shown in Table 2. Particle size is a key indicator of the physiological function of DF. Extrusion processing resulted in the increased SSA and decreased particle size of IDF and SDF compared to those of control IDF and SDF. This was due to the high shear stress during extrusion promoted the collision and friction of particles, and lossened the internal structure of dietary fiber[20]. Partial dietary fiber has been melted due to the heat and strong force of extrusion, which reduced particle size and increased specific surface area[21].

3.3.2 Fourier transform infrared spectroscopy analysis

The FTIR spectra of dietary fiber was shown in Fig. 3A. The absorption peaks of DF showed the typical structure of

Table 2 Particle size analysis and SSA of IDF and SDF

Treatment	$d_{0.1}$ (μm)	$d_{0.5}$ (μm)	$d_{0.9}$ (μm)	D (3,2) (μm)	D (4,3) (μm)	SSA (m^2/g)
RSDF	11.16 ± 0.40^c	28.78 ± 0.10^c	70.44 ± 0.65^c	21.75 ± 0.08^c	38.02 ± 0.40^c	0.276 ± 0.001^b
ESDF	5.25 ± 0.01^d	16.32 ± 0.03^d	43.14 ± 0.08^d	11.37 ± 0.01^d	22.02 ± 0.28^d	0.528 ± 0.001^a
RIDF	12.07 ± 0.04^b	149.08 ± 1.43^a	355.93 ± 3.51^a	32.18 ± 0.19^a	166.39 ± 1.65^a	0.187 ± 0.001^d
EIDF	12.59 ± 0.14^a	84.62 ± 0.00^b	257.99 ± 0.23^b	31.00 ± 0.18^b	113.17 ± 0.07^b	0.194 ± 0.002^c

n=3. Values were expressed mean ± SD. Different letters in the same column indicated significant difference ($P < 0.05$).

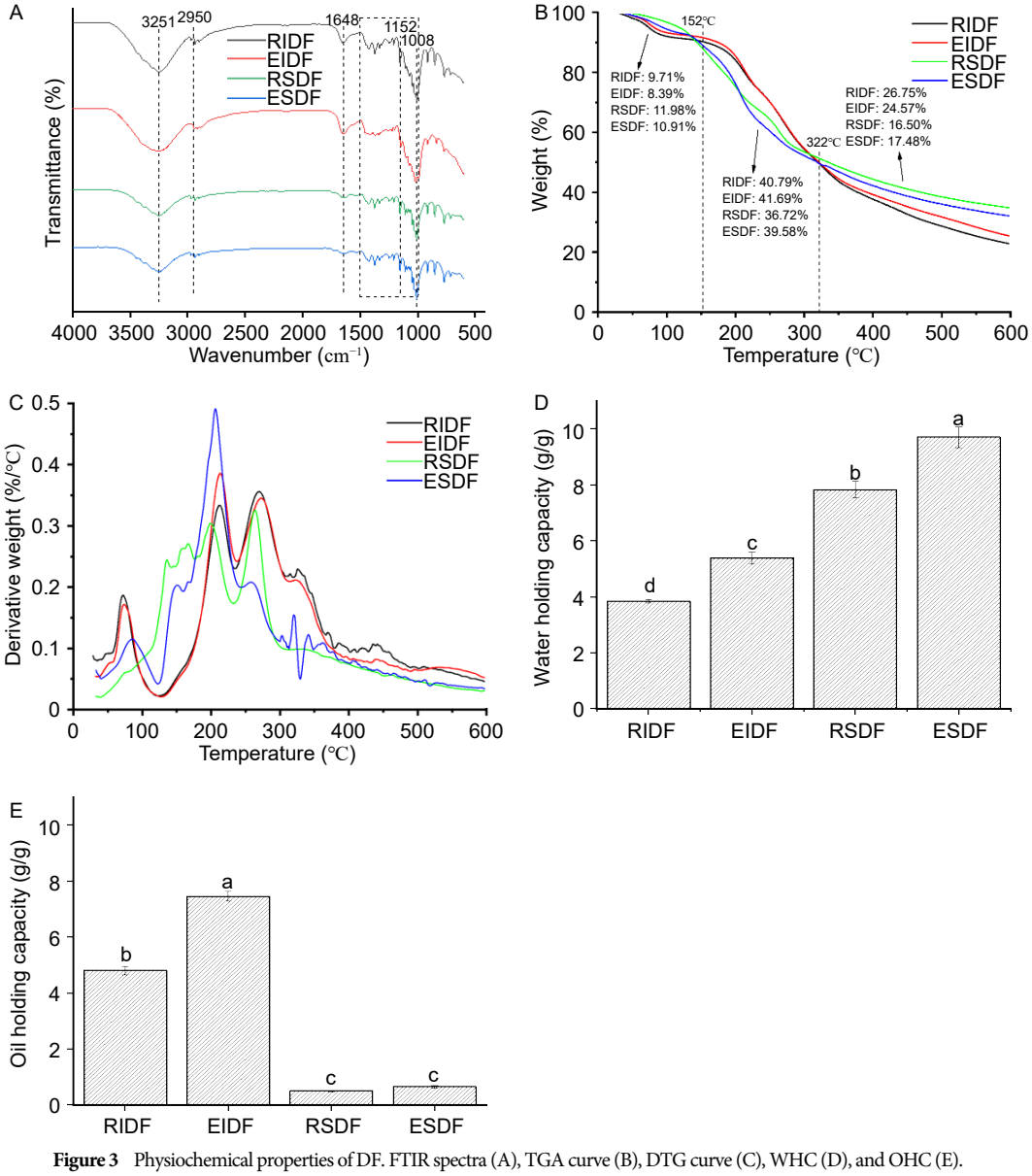

Figure 3 Physiochemical properties of DF. FTIR spectra (A), TGA curve (B), DTG curve (C), WHC (D), and OHC (E).

polysaccharides. The wide absorption band near 3,400 cm^{-1} was attributed to the stretching of -OH mainly from cellulose[2]. EIDF and ESDF showed weakened absorption band after extrusion processing compared to RIDF and RSDF, respectively. This was probably due to the weakened intramolecular hydrogen bonds after extrusion processing, thus increased the number of hydrophilic sites[22,23]. The absorption peak at 2,950 cm^{-1} and 1,000-1,500 cm^{-1} was attributed to C-H stretching vibration and the variable angle vibration of C-H[5]. The peak at 1,658 cm^{-1} was originated from the stretching of C=O. The band at 1,041 cm^{-1} was the stretching vibration of C-O which is a typical absorption peak of xylose[24]. FTIR analysis indicated that cellulose and some reactive groups such as hydroxyl, carbonyl of DF significantly changed after extrusion processing, due to the degradation of macromolecules under mechanical strength[9]. And this result was corresponsive to the monosaccharide composition shown in Table 1.

3.3.3 *Thermogravimetric analysis*

Thermogravimetric analysis of DF can be used to explain the thermal stability and compositional changes as the increase of temperature (Figs. 3B, 3C). A slight decrease in weight of 8.3.9-

11.98% for DF was observed in the initial stage of 28-152 °C due to the evaporation of free water and water adsorbed by hydrophilic groups of fiber. A rapid reduction of sample mass during the second stage of 152-322 °C was observed due to the dehydrogenation, dihydroxylation, and decarboxylation[9, 14]. In the second stage, the mass loss of IDF was higher than that of SDF which was attributed to decomposition of cellulose[25]. In the third stage of 322-600 °C, DF went through the biocarbonization. The residual mass of IDF was lower than that of SDF.

3.3.4 *Water holding capacity and oil holding capacity*

The WHC and OHC of IDF and SDF was shown in Figs. 3B, 3E. WHC and OHC are important physicochemical indicators for food viscosity and prevention of fat loss during food processing, respectively. WHC and OHC of IDF and SDF after extrusion was significantly improved ($P < 0.05$), which was due to the porous structure and increased SSA of SDF and IDF. This result was corresponsive to SEM analysis that porous structure of IDF and SDF after extrusion processing. In addition, SDF showed higher WHC compared to that of IDF ($P < 0.05$). This was attributed to the glycosidic bonds in polysaccharide chains were disrupted during extrusion processing and more hydrophilic/lipophilic groups were exposed on the surface, thus had more water and oil binding sites[26]. DF with high WHC has the potential to avoid synaeresis and modify the viscosity and texture of food[4]. Arabinoxylan in DF was reported to contribute to the absorption of lipids[27]. This was corresponsive to the result of monosaccharide composition of IDF and SDF.

3.4 Functional properties

3.4.1 *Glucose adsorption capacity (GAC) and glucose dialysis retardation index (GDRI)*

GAC was used to assess the ability of DF to adsorb glucose *in vitro*. DF of HB after extrusion processing showed increased GAC compared to that of control IDF and SDF ($P < 0.05$) (Fig. 4A). GAC was increased as the increased concentration of IDF and SDF from 10-200 mmol/L. This was highly related to the increased SSA of IDF and SDF after extrusion processing that more binding sites were exposed for glucose absorption, which resulted in the increased specific surface area[9, 26]. Thus, extrusion processing favored the glucose absorption of IDF and SDF for glucose control. In addition, the SDF showed higher GAC than that of IDF at the same test concentration of glucose.

GDRI is an important *in vitro* indicator to reflect the effect of DF on GI blood glucose. GDRI of DF at time of 30 and 60 min was shown in Fig. 4B. The maximum GDRI was observed at 30 min and tended to be decreased as the time increased up to 60 min. This result was in agreement with Niu *et al.*[9] that the maximum GDRI of DF was observed at 30 min and further declined as time extended. Extrusion processing resulted in the significant increase of GDRI of DF compared to those of control DF ($P < 0.05$). The increased SSA of DF after extrusion processing favored the glucose absorption, thus delayed the glucose diffusion[14]. In addition, SDF showed higher GDRI than that of IDF.

3.4.2 *Inhibitory activities of α-amylase and α-glucosidase*

Inhibitory effect of DF against α-amylase and α-glucosidase was shown in Figs. 4C, 4D. The inhibitory effect of DF against α-amylase and α-glucosidase was closely related to the reduction in postprandial blood glucose level. The inhibitory activity against α-amylase and α-glucosidase of IDF and SDF was increased as the increased concentration of 0.5-6 mg/mL of DF. Extrusion processing improved the inhibitory effect of DF against α-amylase and α-glucosidase compared to those of control DF. Extrusion processing led to the loose and porous structure and increased SSA of DF which improved the formation of physical barriers to restrict glucose diffusion[28, 29]. In addition, SDF showed greater inhibitory activities against α-amylase and α-glucosidase compared to those of IDF.

3.4.3 *Cholesterol adsorption capacity*

CAC of SDF and IDF at pH of 2 and 7 was shown in Fig. 4E. Extrusion processing significantly improved CAC of IDF and SDF at pH 2 and 7 compared to those of control SDF and IDF. The increased porous structure and SSA of IDF and SDF through extrusion processing resulted in more exposure of lipophilic groups that favored the affinity of dietary fiber with oil[29]. CAC of DF at pH 7 was higher than that of DF at pH 2. The similar result was also reported by Wu *et al*[30].

3.4.4 *Nitrate ion adsorption capacity*

NIAC of IDF and SDF at pH of 2 and 7 was shown in Fig. 4F. Nitrite, known as reactive ion, can react with secondary amines and amides under acid condition to form N-nitroso compounds, which are the potential carcinogens to animals and humans[4]. Extrusion processing significantly improved the NIAC of DF at pH of 2 and 7. NIAC of DF was associated with the active groups on the surface of DF and the surface area of DF[14]. Deng *et al.*[31] reported that extrusion processing increased the exposure of carboxyl and hydroxyl groups on the surface of DF, thus increased the adsorption of nitrite ion. Thus, extrusion processing could potentially improve the preventive effect of DF against the development of cancer. In addition, the higher NIAC of dietary fiber at pH of 2 compared to pH of 7 was observed, indicating nitrite ions were primarily absorbed in the stomach. The similar result was also reported by Li *et al.*[16].

3.4.5 *Cation exchange capacity*

CEC of IDF and SDF was shown in Fig. 4G. DF showed cation exchange capacity due to the carboxyl and hydroxyl groups on the surface of DF[30]. Extrusion processing enhanced the CEC of IDF and SDF which was attributed to the increased exposure of ion binding sites on the surface of dietary fiber, thus increased CEC[32]. It also can be explained by extrusion processing resulted in the porous structure and increased specific surface area of dietary fiber which further increased the fluid permeability of dietary fiber, thus favored the CEC of dietary fiber[21].

3.4.6 *Total phenolic content*

TPC in IDF and SDF after extrusion processing was significantly increased (Fig. 5A). This was in agreement with previous study[32]. It has been reported that soluble phenolic compounds could be release through extrusion processing due to high pressure and temperature and mechanical stress[33]. The sample was severely damaged by the extrusion treatment, more reactive sites might be exposed to alkaline solution that hydrolyze the covalent bonds between fibers and phenolics[34].

3.4.7 *Antioxidant activities of SDF and IDF*

DPPH and $ABTS^+$ scavenging ability of DF were shown in Fig. 5. DPPH is used to assess the hydrogen supply capacity of DF as a hydrogen donor. DPPH and $ABTS^+$ scavenging activity of DF

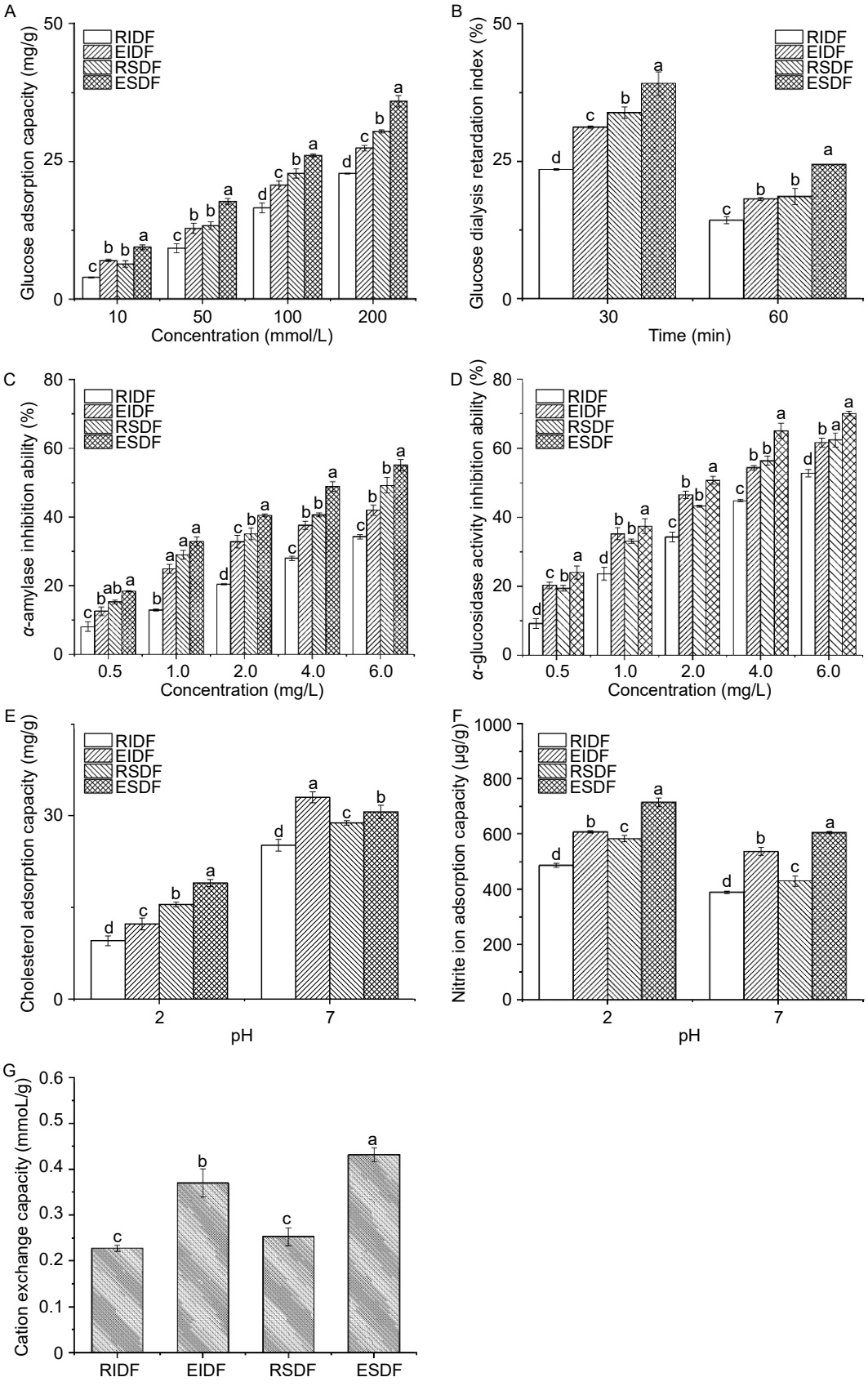

Figure 4 Functional properties. GAC (A), GDRI (B), inhibitory effect against α-amylase (C), inhibitory effect against a-glucosidase (D), CAC (E), NIAC (F), and CEC (G).

was increased as the increased concentration from 0.5-5 mg/mL. DPPH and $ABTS^+$ scavenging ability of IDF and SDF after extrusion was significantly higher than those of control IDF and SDF, respectively ($P < 0.05$). This was in agreement with

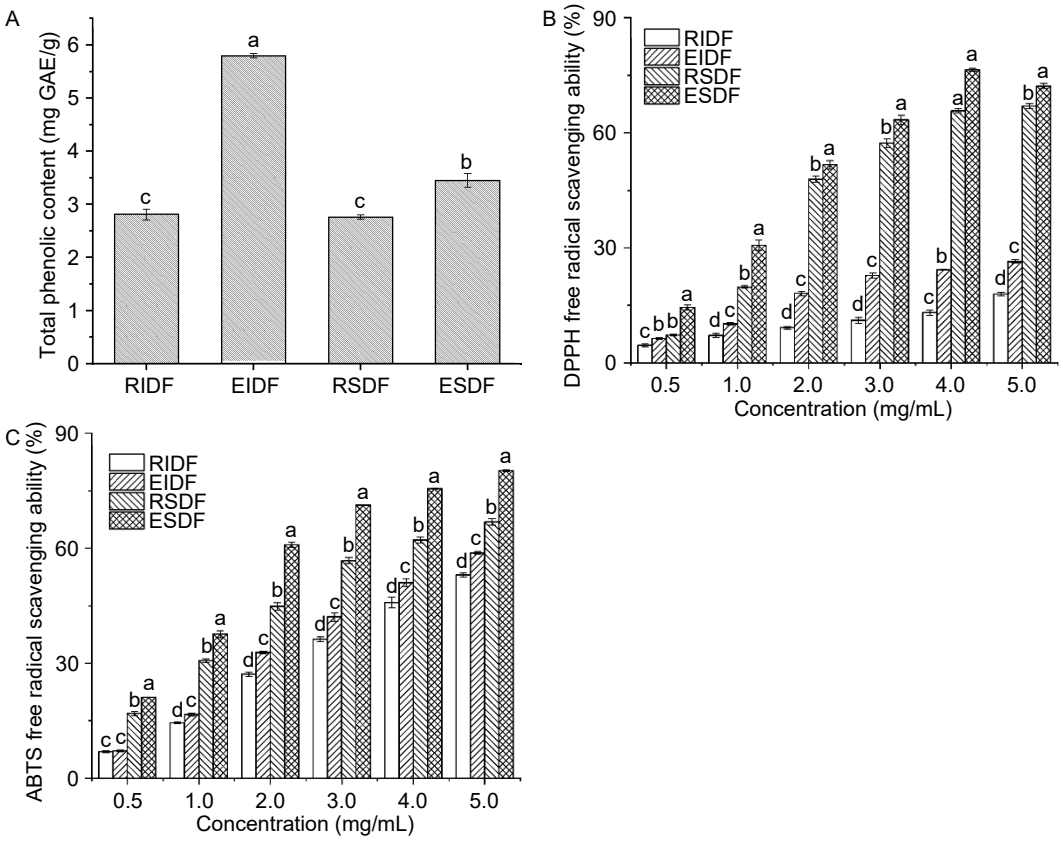

Figure 5 TPC and Antioxidant activities. TPC (A), DPPH free radical scavenging ability (B), and ABTS free radical scavenging ability (C).

Li *et al.*[16]. The increased DPPH scavenging ability of IDF and SDF after extrusion was attributed to the increased SSA of DF due to the effect of extrusion processing[35]. In addition, at the same concentration of IDF and SDF, SDF showed greater DPPH and $ABTS^+$ scavenging abilities than those of IDF. IDF was probably degraded and transferred to SDF through extrusion processing, thus increased the free radical reducing groups such as hydroxyl and amino groups[36].

4 Conclusion

The morphology, physicochemical and functional properties, and antioxidant activities of IDF and SDF of whole grain highland barley before and after extrusion processing were evaluated. Extrusion processing resulted in the loose and porous structure and increased specific surface area of IDF and SDF compared to those of untreated IDF and SDF. WHC and OHC of IDF and SDF were improved by the extrusion processing. Extrusion processing also enhanced the functional properties of dietary fiber such as glucose absorption capacity, glucose dialysis retardation index, inhibitory effect against α-amylase and α-glucosidase, cholesterol absorption capacity, nitrite ion absorption capacity, and cation exchange capacity. The improved functional properties of dietary fiber after extrusion processing can be further evaluated through *in vivo* studies for better understanding the health benefits of dietary fiber. Antioxidant activities including DPPH and $ABTS^+$ scavenging abilities of IDF and SDF were also improved through extrusion processing. Extrusion processing showed the great potential to improve the functional characteristics and antioxidant activities of dietary fiber of whole grain highland barley for the future applications in functional foods.

Conflicts of interest

The authors declare that there are no conflicts of interest in this work.

Acknowledgements

This work was supported by Science and Technology Commission of Shanghai Municipality (No. 23YF1416700) and Shanghai Ocean University.

References

[1] Ramos, S., Martín, M. Á. Impact of diet on gut microbiota. *Current Opinion in Food Science*, **2021**, 37: 83–90. https://doi.org/10.1016/j.cofs.2020.09.006

[2] Xi, H., Wang, A., Qin, W., et al. The structural and functional properties of dietary fibre extracts obtained from highland barley bran through different steam explosion-assisted treatments. *Food Chemistry*, **2023**, 406: 135025. https://doi.org/10.1016/j.foodchem.2022.135025

[3] Obadi, M., Sun, J., Xu, B. Highland barley: chemical composition, bioactive compounds, health effects, and applications. *Food Research International*, **2021**, 140: 110065. https://doi.org/10.1016/j.foodres.2020.110065

[4] Chu, J., Zhao, H., Lu, Z., et al. Improved physicochemical and functional properties of dietary fiber from millet bran fermented by *Bacillus Natto*. *Food Chemistry*, **2019**, 294: 79–86. https://doi.org/10.1016/j.foodchem.2019.05.035

[5] Leonard, W., Zhang, P., Ying, D., et al. Application of extrusion technology in plant food processing byproducts: An overview. *Comprehensive Reviews in Food Science and Food Safety*, **2020**, 19: 218–246. https://doi.org/10.1111/1541-4337.12514

[6] Ge, F., Sun, Y., Yang, C., et al. Exploring the relationship between

starch structure and physicochemical properties: the impact of extrusion on highland barley flour. *Food Research International*, **2024**, 183: 114226. https://doi.org/10.1016/j.foodres.2024.114226

[7] Benítez, V., Rebollo-Hernanz, M., Braojos, C., et al. Changes in the cocoa shell dietary fiber and phenolic compounds after extrusion determine its functional and physiological properties. *Current Research in Food Science*, **2023**, 6: 100516. https://doi.org/10.1016/j.crfs.2023.100516

[8] Li, J., Xi, H., Wang, A., et al. Effects of high-pressure microfluidization treatment on the structural, physiochemical properties of insoluble dietary fiber in highland barley bran. *International Journal of Biological Macromolecules*, **2024**, 262: 129743. https://doi.org/10.1016/j.ijbiomac.2024.129743

[9] Niu, L., Guo, Q., Xiao, J., et al. The effect of ball milling on the structure, physicochemical and functional properties of insoluble dietary fiber from three grain bran. *Food Research International*, **2023**, 163: 112263. https://doi.org/10.1016/j.foodres.2022.112263

[10] Zheng, Y., Wang, X., Tian, H., et al. Effect of four modification methods on adsorption capacities and *in vitro* hypoglycemic properties of millet bran dietary fibre. *Food Research International*, **2021**, 147: 110565. https://doi.org/10.1016/j.foodres.2021.110565

[11] Gu, M., Fang, H., Gao, Y., et al. Characterization of enzymatic modified soluble dietary fiber from tomato peels with high release of lycopene. *Food Hydrocolloids*, **2020**, 99: 105321. https://doi.org/10.1016/j.foodhyd.2019.105321

[12] Chen, H., Xiong, M., Bai, T., et al. Comparative study on the structure, physicochemical, and functional properties of dietary fiber extracts from quinoa and wheat. *LWT-Food Science and Technology*, **2021**, 149: 111816. https://doi.org/10.1016/j.lwt.2021.111816

[13] Zheng, Y., Li, J., Wang, X., et al. Effects of three biological combined with chemical methods on the microstructure, physicochemical properties and antioxidant activity of millet bran dietary fibre. *Food Chemistry*, **2023**, 411: 135503. https://doi.org/10.1016/j.foodchem.2023.135503

[14] Yan, K., Liu, J., Yan, W., et al. Effects of alkaline hydrogen peroxide and cellulase modifications on the physicochemical and functional properties of forsythia suspensa dietary fiber. *Molecules*, **2023**, 28: 7164. https://doi.org/10.3390/molecules28207164

[15] Li, Y., Zhang, Y., Dong, L., et al. Fermentation of *Lactobacillus Fermentum* NB02 with feruloyl esterase production increases the phenolic compounds content and antioxidant properties of oat bran. *Food Chemistry*, **2024**, 437: 137834. https://doi.org/10.1016/j.foodchem.2023.137834

[16] Li, S., Hu, N., Zhu, J., et al. Influence of modification methods on physicochemical and structural properties of soluble dietary fiber from corn bran. *Food Chemistry: X*, **2022**, 14: 100298. https://doi.org/10.1016/j.fochx.2022.100298

[17] Padayachee, A., Day, L., Howell, K., et al. Complexity and health functionality of plant cell wall fibers from fruits and vegetables. *Critical Reviews in Food Science and Nutrition*, **2017**, 57: 59–81. https://doi.org/10.1080/10408398.2013.850652

[18] Ciudad-Mulero, M., Fernández-Ruiz, V., Matallana-González, M. C., et al. Dietary fiber sources and human benefits: The case study of cereal and pseudocereals. *Advances in Food and Nutrition Research*, **2019**, 90: 83–134. https://doi.org/10.1016/bs.afnr.2019.02.002

[19] Ma, Z. Q., Zhang, N., Zhai, X. T., et al. Structural, physicochemical and functional properties of dietary fiber from brown rice products treated by different processing techniques. *LWT-Food Science and Technology*, **2023**, 182: 114789. https://doi.org/10.1016/j.lwt.2023.114789

[20] Yang, M., Wu, L., Cao, C., et al. Extrusion improved the physical and chemical properties of dietary fibre from bamboo shoot by-products. *International Journal of Food Science & Technology*, **2021**, 56: 847–856. https://doi.org/10.1111/ijfs.14728

[21] Yan, J., Li, Y., Bai, S., et al. Comparison of structural, physicochemical and functional properties of dried coconut dietary fiber by steam explosion and extrusion modification. *Industrial Crops and Products*, **2024**, 218: 118916. https://doi.org/10.1016/j.indcrop.2024.118916

[22] Bai, Y. P., Zhou, H. M., Zhu, K. R., et al. Effect of thermal processing on the molecular, structural, and antioxidant characteristics of highland barley *β*-glucan. *Carbohydrate Polymers*, **2021**, 271: 118416. https://doi.org/10.1016/j.carbpol.2021.118416

[23] Qiao, H., Shao, H., Zheng, X., et al. Modification of sweet potato (*Ipomoea Batatas* Lam.) residues soluble dietary fiber following twin-screw extrusion. *Food Chemistry*, **2021**, 335: 127522. https://doi.org/10.1016/j.foodchem.2020.127522

[24] Wang, K., Li, M., Wang, Y., et al. Effects of extraction methods on the structural characteristics and functional properties of dietary fiber extracted from kiwifruit (*Actinidia Deliciosa*). *Food Hydrocolloids*, **2021**, 110: 106162. https://doi.org/10.1016/j.foodhyd.2020.106162

[25] Huang, J., Liao, J., Qi, J., et al. Structural and physicochemical properties of pectin-rich dietary fiber prepared from citrus peel. *Food Hydrocolloids*, **2021**, 110: 106140. https://doi.org/10.1016/j.foodhyd.2020.106140

[26] Ma, Q., Yu, Y., Zhou, Z., et al. Effects of different treatments on composition, physicochemical and biological properties of soluble dietary fiber in buckwheat bran. *Food Bioscience*, **2023**, 53: 102517. https://doi.org/10.1016/j.fbio.2023.102517

[27] Devi, P. B., Vijayabharathi, R., Sathyabama, S., et al. Health benefits of finger millet (*Eleusine Coracana* L.) polyphenols and dietary fiber: A review. *Journal of Food Science and Technology*, **2014**, 51: 1021–1040. https://doi.org/10.1007/s13197-011-0584-9

[28] Zhang, H., Sun, S., Ai, L. Physical barrier effects of dietary fibers on lowering starch digestibility. *Current Opinion in Food Science*, **2022**, 48: 100940. https://doi.org/10.1016/j.cofs.2022.100940

[29] Jiang, C., Zeng, X., Wei, X., et al. Improvement of the functional properties of insoluble dietary fiber from corn bran by ultrasonic-microwave synergistic modification. *Ultrasonics Sonochemistry*, **2024**, 104: 106817. https://doi.org/10.1016/j.ultsonch.2024.106817

[30] Wu, Q., Zhang, M., Hu, H., et al. Comparative study on chemical composition, functional properties of dietary fibers prepared from four China cereal brans. *International Journal of Biological Macromolecules*, **2024**, 257: 128510. https://doi.org/10.1016/j.ijbiomac.2023.128510

[31] Deng, M., Lin, Y., Dong, L., et al. Physicochemical and functional properties of dietary fiber from pummelo (*Citrus Grandis* L. Osbeck) and grapefruit (*Citrus Paradisi* Mcfad) cultivars. *Food Bioscience*, **2021**, 40: 100890. https://doi.org/10.1016/j.fbio.2021.100890

[32] Ma, Q., Ma, Z., Wang, W., et al. The effects of enzymatic modification on the functional ingredient - dietary fiber extracted from potato residue. *LWT-Food Science and Technology*, **2022**, 153: 112511. https://doi.org/10.1016/j.lwt.2021.112511

[33] Jan, R., Saxena, D. C., Singh, S. Effect of extrusion variables on antioxidant activity, total phenolic content and dietary fibre content of gluten-free extrudate from germinated chenopodium (*Chenopodium Album*) flour. *International Journal of Food Science & Technology*, **2017**, 52: 2623–2630. https://doi.org/10.1111/ijfs.13549

[34] Chen, Y., Ma, Y., Dong, L., et al. Extrusion and fungal fermentation change the profile and antioxidant activity of free and bound phenolics in rice bran together with the phenolic bioaccessibility. *LWT-Food Science and Technology*, **2019**, 115: 108461. https://doi.org/10.1016/j.lwt.2019.108461

[35] Zhong, L., Fang, Z., Wahlqvist, M. L., et al. Multi-response surface optimisation of extrusion cooking to increase soluble dietary fibre and polyphenols in lupin seed coat. *LWT-Food Science and Technology*, **2021**, 140: 110767. https://doi.org/10.1016/j.lwt.2020.110767

[36] Xiong, M., Zheng, S., Bai, T., et al. The difference among structure, physicochemical and functional properties of dietary fiber extracted from triticale and hull-less barley. *LWT-Food Science and Technology*, **2022**, 154: 112771. https://doi.org/10.1016/j.lwt.2021.112771